Effect of Rosiglitazone on Bone Quality in a Rat Model of Insulin Resistance and Osteoporosis

Laura D. Sardone,[1,2] Richard Renlund,[3] Thomas L. Willett,[2,3] Ivan G. Fantus,[2,4] and Marc D. Grynpas[1,2]

OBJECTIVE—Rosiglitazone (RSG) is an insulin-sensitizing drug used to treat type 2 diabetes mellitus. The A Diabetes Outcome Progression Trial (ADOPT) shows that women taking RSG experienced more fractures than patients taking other type 2 diabetes drugs. These were not osteoporotic vertebral fractures but, rather, occurred in the limbs. The purpose of this study was to investigate how RSG treatment alters bone quality, which leads to fracture risk, using the Zucker fatty rat as a model.

RESEARCH DESIGN AND METHODS—A total of 61 female 4-month-old rats were divided into six groups. One Sham group was a control and another was administered oral RSG 10 mg/kg/day. Four ovariectomized (OVX) groups were dosed as follows: controls, RSG 10 mg/kg, alendronate (ALN, injected at 0.7 mg/kg/week), and RSG 10 mg/kg plus ALN. After 12 weeks of treatment, bone quality was evaluated by mechanical testing. Microarchitecture, bone mineral density (BMD), cortical bone porosity, and bone remodeling were also measured.

RESULTS—OVX RSG 10 mg/kg rats had lower vertebral BMD and compromised trabecular architecture versus OVX controls. Increased cortical bone porosity and decreased mechanical properties occurred in these rats. ALN treatment prevented decreased BMD and architectural and mechanical properties in the OVX model. Reduced bone formation, increased marrow adiposity, and excess bone resorption were observed in RSG-treated rats.

CONCLUSIONS—RSG decreases bone quality. An unusual finding was an increase in cortical bone porosity induced by RSG, consistent with its effect on long bones of women. ALN, an inhibitor of bone resorption, enhanced mechanical strength and may provide an approach to partially counter the deleterious skeletal effects of RSG. ***Diabetes*** **60:3271–3278, 2011**

Type 2 diabetes mellitus is becoming increasingly prevalent (1), creating a demand for drug therapy when lifestyle and dietary changes are not sufficient. Thiazolidinediones (TZDs) are a recently introduced class of oral antidiabetes agents to treat the symptoms of type 2 diabetes (2). Rosiglitazone (RSG), a member of the TZD class of drugs, is an insulin sensitizer that improves glycemic control (3). Although TZDs are effective in type 2 diabetes, these drugs have been associated with adverse skeletal effects, especially in older females (4–7).

This was shown in the A Diabetes Outcome Progression Trial (ADOPT), in which female patients taking RSG experienced more fractures than patients taking other type 2 diabetes drugs (5,8). These were not the usual osteoporotic fractures of the spine and hip but, rather, occurred in the upper and lower limbs. The increase in fractures was significant in women but not in men. Bone loss after RSG treatment has also been documented in mice and rats (9,10).

RSG is an agonist for the peroxisome proliferator–activated receptor-γ (PPAR-γ) (11–15). Activation of this receptor by RSG allows for the regulation of insulin-responsive genes (10). It also stimulates mesenchymal cells to preferentially differentiate into marrow adipocytes as opposed to osteoblasts (16). Therefore, there is concern regarding the skeletal effects of RSG in type 2 diabetic subjects. It is interesting that a complication of type 2 diabetes is an increased risk of osteoporotic fractures despite elevated bone mineral density (BMD) (17). Various risk factors may contribute to this risk, such as abnormal insulin levels, hypercalciuria, advanced glycation end products, inflammation, lower levels of insulin-like growth factor I, and reduced renal function (17).

In vitro studies report a decrease in bone formation due to increased adipogenesis at the expense of osteoblastogenesis (16). In vivo studies are less conclusive, with evidence supporting both decreased bone formation and increased resorption. RSG has been shown to decrease BMD and trabecular structural properties, as well as osteoblast number, while simultaneously increasing fat content (18). Other studies, however, suggest that activation of PPAR-γ by RSG regulates osteoclastogenesis in vivo, which would affect bone resorption (19). Increased osteoclast number and eroded surface (ES) were observed in ovariectomized (OVX) rats after RSG treatment (20). Furthermore, bone loss in vivo induced by RSG was associated with increased osteoclastogenesis (21,22).

Maintaining a balance between bone formation by osteoblasts and bone resorption by osteoclasts is imperative for a healthy skeleton (23). The bone remodeling process is a major determinant of fracture risk, and an imbalance can lead to osteoporosis (24). Postmenopausal estrogen deficiency causes an increased rate of bone turnover leading to decreased bone mass. In the aged rat model, estrogen deficiency induced by ovariectomy causes increased bone turnover and an excess of bone resorption (25). Bisphosphonates, such as alendronate (ALN), are commonly prescribed treatments for osteoporosis owing to their antiresorptive effects (26).

In this study, to represent the clinical context in which the adverse effects of RSG on bone have been observed, we assessed its effects on bone loss and bone quality in both Sham and OVX Zucker fatty (ZF) rats, a model of obesity and insulin resistance (27). The ZF rat is characterized by

From the [1]Department of Laboratory Medicine and Pathobiology, University of Toronto, Toronto, Ontario, Canada; the [2]Samuel Lunenfeld Research Institute, Mount Sinai Hospital, Toronto, Ontario, Canada; the [3]Department of Surgery, University of Toronto, Toronto, Ontario, Canada; and the [4]Department of Medicine, Mount Sinai Hospital, University of Toronto, Toronto, Ontario, Canada.

Corresponding author: Marc D. Grynpas, grynpas@lunenfeld.ca.

Received 10 December 2010 and accepted 20 August 2011.

DOI: 10.2337/db10-1672

This article contains Supplementary Data online at http://diabetes.diabetesjournals.org/lookup/suppl/doi:10.2337/db10-1672/-/DC1.

hyperinsulinemia, hyperlipidemia, mild hyperglycemia, and insulin resistance (28–31). We sought to determine if RSG treatment enhances the changes in bone quality (structural, mechanical, and histological properties) that occur in the estrogen-deficient state and whether the administration of ALN could inhibit these actions.

RESEARCH DESIGN AND METHODS

Animal husbandry. A total of 61 female ZF rats (*fa/fa*), aged 16 weeks, were purchased from Charles River (Senneville, Quebec, Canada). All rats were housed singly on cornmeal bedding in plastic cages that contained a hide-away tube. The rats were fed and watered ad lib and aged for 9 weeks prior to treatment. During this period, all rats received a 1 ml piece of artificially sweetened strawberry Jell-O 5 days a week. Select groups were ovariectomized at age 16 weeks (Table 1). All procedures were carried out in accordance with the Canadian Council of Animal Care guidelines and were approved by the University of Toronto Animal Care Committee.

RSG and ALN treatment. The rats were divided into treatment groups described in Table 1. RSG was administered in the Jell-O 5 days a week for 12 weeks. ALN was administered via subcutaneous injection once a week for 12 weeks. At 12 days and 2 days prior to killing, all rats were injected with Calcein Green, a bone mineralization marker (32). After 12 weeks of treatment, all rats were killed. The right and left femora and the L5 and L6 lumbar vertebrae were dissected and kept moist with saline-soaked gauze. These specimens were stored at −20°C and were thawed at room temperature prior to testing. The right tibiae were dissected and immediately fixed in 70% ethanol in preparation for embedding for histomorphometry.

Evaluation of BMD and architecture. Dual-energy X-ray absorptiometry (DEXA) was performed on all right femora and L5 and L6 lumbar vertebrae to determine BMD (33). This method generates a two-dimensional measurement of BMD using a small animal densitometer (PIXImus; GE, Mississauga, Ontario, Canada), which was calibrated with an aluminum/leucite phantom (33).

Microcomputed tomography (MicroCT) was performed on all right femora and L6 lumbar vertebrae providing a three-dimensional measurement of BMD and bone architecture (34). Analysis of L6 vertebrae yielded measurements of percent trabecular bone volume (BV), trabecular thickness, trabecular number, and trabecular separation. Analysis of right femora yielded measurements for anterior/posterior diameter, medial/lateral diameter, polar moment of inertia (mm^4), cross-sectional area (mm^2), and elliptical moment of inertia (mm^4) (34). These femoral parameters were used to normalize the results from three-point bending and torsion testing. MicroCT was also used to assess the total porosity (percent) for all right femora.

Mechanical testing. To evaluate the mechanical properties of cortical bone, right femora were tested in three-point bending, and the diaphyses of left femora were tested in torsion. To evaluate the mechanical properties of trabecular bone, all proximal halves of right femora were tested in femoral neck fracture and all L6 vertebrae were tested in vertebral compression. For three-point bending, a preload between 1 and 2 N was applied to the midpoint of the right diaphysis, and the bone was loaded in bending until failure at a rate of 1 mm/min using an Instron 4465 (Instron, Norwood, MA) with a 1,000-N load cell as previously described (35). For femoral neck fracture testing, a preload between 0.5 and 1 N was applied and the femoral head was loaded until failure at 2.5 mm/min (36). For torsion testing, left femur diaphyses were tested on a custom built machine with a 20–lb-in load cell until failure at a speed of 1.5 degrees/sec as previously described (35). L6 lumbar vertebrae were tested in compression using an Instron 4465 as previously described (37). A preload of 5 N was applied, and the vertebra was loaded until failure at a rate of 1 mm/min.

Load-displacement curves were generated using LabView 5.0 software (National Instruments, Austin, TX) to calculate the bone structural properties (38). The ultimate load represents the maximum load that the specimen sustains. The stiffness is determined from the slope of the elastic region of the curve and represents the extrinsic stiffness or the rigidity of the specimen. The failure displacement measures the extent of deformation of the bone at failure, and the energy to failure represents the amount of energy that the specimen can absorb prior to breaking (38).

Three-point bending, torsion, and vertebral compression data were normalized using the geometrical measurements to generate a stress-strain curve and to determine the material properties (ultimate stress, modulus, and toughness) of the bones (39,40). Femoral neck fracture data cannot be normalized as a result of the complex geometry of the femoral head/neck.

Specimen processing and histomorphometry. After dissection, all right tibiae were cut in half, and each proximal half was cut coronally using an Isomet low speed saw (Buehler, Whitby, Ontario, Canada). Proximal cranial halves of right tibiae were then fixed in 70% ethanol for 1 week, followed by dehydration in acetone and infiltration with Spurr resin. Specimens were then embedded in Spurr resin and polymerized. The Spurr blocks containing the tibia samples were sectioned into 5-μm sections (Leica RM2265 microtome; Leica Microsystems, Richmond Hill, Ontario, Canada) for static histomorphometry and 7-μm sections for dynamic histomorphometry. The 5-μm sections were stained with Goldner's Trichrome (41). The region of interest was located 1 mm distal to the tibial growth plate to ensure that only trabecular bone was being analyzed. Using a magnification of ×100, four fields were analyzed using an image analysis system (Bioquant Nova Prime, version 6.50.10; Bioquant, Nashville, TN) to obtain the following parameters: osteoid surface/bone surface (OS/BS), osteoid volume/BV (OV/BV), and ES.

Dynamic histomorphometry was performed on unstained 7-μm sections using the same tibial region of interest as in static histomorphometry. Sections were analyzed under ultraviolet light for Calcein Green labeling (41). Using a magnification of ×100, four fields were analyzed using Bioquant image analysis system to obtain bone formation parameters, including mineralized surface/BS (MS/BS) and bone formation rate (BFR). All measurements were completed following the nomenclature and guidelines from the American Society for Bone and Mineral Research (42).

Statistical analysis. SPSS version 17.0 software (SPSS, Inc., Chicago, IL) was used to perform statistical analysis. Student *t* test was used to evaluate differences between the two female Sham groups and between the female Sham control and OVX control groups. For the female OVX study, a two-way ANOVA was used to determine if there were any differences in means among the two treatments (RSG and ALN) and to determine if there was any interaction between the two drugs. Multiple comparisons were performed using Fisher least significant differences post hoc test. $P < 0.05$ was accepted as significant. Data are presented as mean ± SD.

TABLE 1
Treatment groups for 61 ZF rats

Group	Rats (*n*)	Model	Treatment
1	9	ZF sham	Vehicle
2	8	ZF sham	RSG 10 mg/kg
3	9	ZF OVX	Vehicle
4	12	ZF OVX	ALN 0.7 mg/kg
5	11	ZF OVX	RSG 10 mg/kg
6	12	ZF OVX	RSG 10 mg/kg + ALN 0.7 mg/kg

RESULTS

The effect of RSG on BMD in the ZF OVX model. Results from DEXA and MicroCT analysis can be found in Table 2. DEXA and MicroCT analysis both confirmed the effect of OVX in the ZF rat model. OVX controls showed significantly lower vertebral aerial and volumetric BMD than Sham controls ($P < 0.05$) as expected after OVX. The OVX RSG group demonstrated significantly lower vertebral aerial and volumetric BMD ($P < 0.05$) compared with OVX controls and the OVX ALN group. Both OVX ALN–treated groups showed significantly increased vertebral aerial and volumetric BMD compared with OVX controls and OVX RSG groups ($P < 0.05$). In the case of vertebral volumetric BMD, ALN may be attenuating the effects of RSG because there was only a 5% decrease in BMD from the OVX ALN to the OVX RSG plus ALN group compared with a 15% decrease in BMD from OVX controls to the OVX RSG group.

OVX controls showed significantly lower femoral aerial BMD than Sham controls ($P < 0.05$). The OVX RSG group demonstrated significantly lower femoral aerial BMD ($P < 0.05$) compared with OVX controls. Both OVX ALN–treated groups showed significantly increased femoral aerial and volumetric BMD compared with OVX controls and OVX RSG groups ($P < 0.05$). However, there were no differences when comparing femoral volumetric BMD of the OVX RSG group to the other OVX groups.

The effect of RSG on bone structural properties. Trabecular architecture properties, as analyzed by MicroCT, can be found in Table 3. The OVX control group demonstrated

TABLE 2
Aerial and volumetric BMD for all groups

	Sham		OVX			
BMD	Control	RSG 10	Control	RSG 10	ALN	RSG 10 + ALN
Femoral (g/cm^2)	0.20 ± 0.01	0.20 ± 0.01	**0.19 ± 0.01**^{g}	**0.18 ± 0.01**^{de}	**0.22 ± 0.01**^{df}	**0.21 ± 0.00**^{d}
Vertebral (g/cm^2)	0.11 ± 0.01	0.11 ± 0.01	**0.10 ± 0.01**^{g}	**0.09 ± 0.01**^{d}	**0.13 ± 0.01**^{df}	**0.12 ± 0.01**^{d}
Femoral volumetric	1.16 ± 0.03	1.16 ± 0.01	1.15 ± 0.02	1.15 ± 0.01	1.16 ± 0.01	**1.17 ± 0.01**^{f}
Vertebral volumetric	0.57 ± 0.06	0.54 ± 0.02	**0.52 ± 0.06**^{g}	**0.44 ± 0.04**^{de}	**0.62 ± 0.05**^{df}	**0.59 ± 0.04**^{df}

Data are presented as mean ± SD. Boldface indicates significance. ^{d}Indicates significance vs. OVX controls ($P < 0.05$). ^{e}Indicates significance vs. OVX ALN group ($P < 0.05$). ^{f}Indicates significance vs. OVX RSG 10 mg/kg group ($P < 0.05$). ^{g}Indicates significance vs. Sham control group ($P < 0.05$).

significantly decreased trabecular percent BV and trabecular number and increased trabecular separation compared with Sham controls. RSG treatment resulted in further decreased percent BV, trabecular thickness, and trabecular number and increased trabecular separation compared with the OVX control group ($P < 0.05$). The OVX ALN groups, with or without RSG, showed the opposite result with increased percent BV and increased trabecular number compared with the OVX controls and OVX RSG groups ($P < 0.05$).

Porosity measurements. The results from porosity measurements via MicroCT can be found in Table 4 and Fig. 1. The OVX RSG group demonstrated significantly higher femoral total porosity than OVX controls ($P = 0.023$). Both OVX ALN groups had significantly lower total porosity than the OVX RSG group ($P < 0.05$). However, it should be noted that RSG did increase cortical porosity in the presence and absence of ALN.

The effect of RSG on mechanical properties of cortical bone. After mechanical testing of cortical bone, there were no significant differences in any parameters between the Sham controls and OVX controls. Results from all mechanical testing can be found in Table 5. In three-point bending, ALN treatment increased mechanical strength relative to RSG-treated groups. The OVX RSG plus ALN group showed significantly higher ultimate load and failure load compared with the OVX RSG group ($P < 0.05$) (Table 5). Once data were normalized, the OVX RSG plus ALN group demonstrated significantly higher ultimate stress and toughness than the OVX RSG group ($P < 0.05$) (Supplementary Table 1). Also, these values for ultimate stress and toughness were not decreased compared with the OVX ALN group, suggesting that ALN is protecting against the effects of RSG in three-point bending testing.

After torsion testing of left femora, the OVX RSG group demonstrated significantly lower failure torque and torsional stiffness compared with OVX controls ($P < 0.05$) (Table 5). Of interest, the OVX RSG plus ALN group also demonstrated lower failure torque and stiffness compared with OVX controls and the OVX ALN group ($P < 0.05$) (Table 5), suggesting that ALN cannot protect against the effects of RSG in torsion. Once data were normalized, the OVX RSG group showed significantly decreased shear stress and shear modulus compared with OVX controls ($P < 0.05$) (Supplementary Table 1). The OVX RSG plus ALN group demonstrated decreased shear stress compared with the OVX ALN group ($P < 0.05$) (Supplementary Table 1), again suggesting that the presence of ALN does not protect against the effects of RSG in this parameter.

The effect of RSG on mechanical properties of trabecular bone. There were no significant differences between the Sham controls and OVX controls for any of the parameters from vertebral compression testing of all L6 vertebrae (Supplementary Table 1). The OVX RSG group showed significantly decreased ultimate load compared with OVX controls ($P < 0.05$) (Table 5). Both OVX ALN groups had significantly higher ultimate load compared with OVX controls. The OVX ALN also had significantly increased stiffness compared with OVX controls (Table 5). Once normalized, the OVX RSG group demonstrated significantly decreased ultimate stress and toughness compared with OVX controls ($P < 0.05$) (Supplementary Table 1). The OVX RSG plus ALN group had significantly increased ultimate stress compared with OVX RSG groups ($P < 0.05$) (Supplementary Table 1).

After femoral neck fracture testing on all proximal femora, the OVX RSG group showed significantly decreased ultimate load compared with OVX controls ($P < 0.05$) (Table 5). The OVX RSG plus ALN group showed significantly increased ultimate load and energy to failure compared with the OVX RSG group ($P < 0.05$) (Table 5). In this case, ALN treatment largely reverses the adverse effects of RSG. In the presence of ALN, RSG does not cause the decrease in ultimate load that is observed in the absence of ALN.

The effect of RSG on bone remodeling. Results from static and dynamic histomorphometry can be found in Table 6. Static histomorphometry analysis revealed significantly lower

TABLE 3
MicroCT results for trabecular bone for all groups

	Sham		OVX			
	Control	RSG 10	Control	RSG 10	ALN	RSG 10 + ALN
BV (%)	39.54 ± 4.78	37.25 ± 2.12	34.46 ± 4.75	**28.17 ± 3.73**^{de}	**43.17 ± 4.38**^{d}	**40.67 ± 3.44**^{df}
Trabecular bone						
Thickness	0.11 ± 0.01	0.11 ± 0.00	0.11 ± 0.01	**0.10 ± 0.01**^{de}	0.11 ± 0.00	0.11 ± 0.00
Number	3.54 ± 0.27	3.54 ± 0.14	3.13 ± 0.30	**2.82 ± 0.23**^{de}	**3.83 ± 0.33**^{d}	**3.67 ± 0.21**^{df}
Separation	0.20 ± 0.03	0.22 ± 0.01	0.24 ± 0.02	**0.27 ± 0.02**^{de}	**0.20 ± 0.02**^{d}	0.21 ± 0.02

Data are presented as mean ± SD. Boldface indicates significance. ^{d}Indicates significance vs. OVX controls ($P < 0.05$). ^{e}Indicates significance vs. OVX ALN group ($P < 0.05$). ^{f}Indicates significance vs. OVX RSG 10 mg/kg group ($P < 0.05$).

TABLE 4
Total porosity for all groups

	Sham		OVX			
	Control	RSG 10	Control	RSG 10	ALN	RSG 10 + ALN
Porosity (%)	1.29 ± 1.23	0.75 ± 0.57	1.08 ± 0.93	**2.20 ± 1.41**[d]	**0.57 ± 0.53**[f]	**1.1 ± 1.46**[f]

Data are presented as mean ± SD. Boldface indicates significance. [d]Indicates significance vs. OVX controls ($P < 0.05$). [f]Indicates significance vs. OVX RSG 10 mg/kg group ($P < 0.05$).

percent OV/BV and percent OS/BS for the OVX RSG group compared with OVX controls ($P < 0.05$), suggesting impaired bone formation with RSG treatment. In addition, both OVX ALN groups showed decreased percent OV/BV and percent OS/BS compared with OVX controls ($P < 0.05$), which is expected after chronic usage of bisphosphonates. We also observed an increase in ES, an indicator of increased bone resorption, which was significant in the OVX RSG group compared with OVX controls ($P < 0.05$). RSG treatment also appeared to result in increased adiposity (Fig. 2), which was consistently observed in all RSG-treated tibiae.

After dynamic histomorphometry, OVX controls showed significantly increased percent MS compared with Sham controls ($P < 0.05$). The OVX RSG group showed significantly

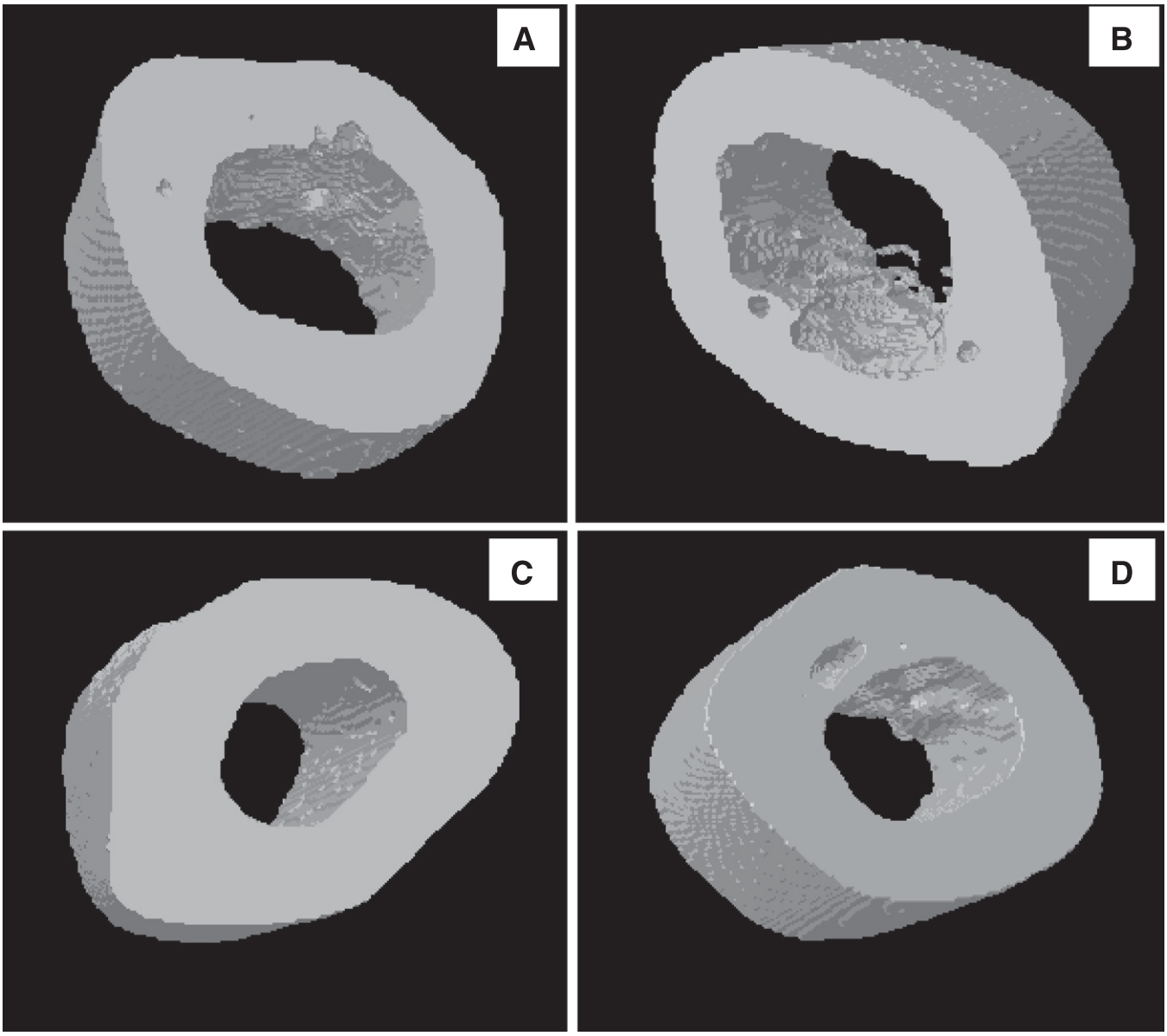

FIG. 1. Representative three-dimensional images showing porosity in cross sections of rat femora obtained with MicroCT. Porosity analysis showed a significant increase in femoral porosity for OVX rats treated with an RSG dose of 10 mg/kg ($P = 0.023$): OVX controls (*A*), OVX RSG 10 (*B*), OVX ALN (*C*), and OVX RSG 10 + ALN (*D*).

decreased MS compared with OVX controls ($P < 0.05$). This group also demonstrated significantly lower BFR compared with OVX controls ($P < 0.05$). All bisphosphonates, including ALN, will eventually reduce bone formation to a very large extent (from 70 to 90%) as a result of their suppression of bone resorption, and this is likely the reason why we were not able to measure BFR (labeling) in the ALN-treated rats (43–45).

DISCUSSION

This study examines the effects of RSG on bone quality in an obese, hyperglycemic, and hyperinsulinemic animal model of type 2 diabetes and osteoporosis. Previous studies examine the effect of RSG on bone loss and bone formation/resorption, but none relate bone structure and composition to bone quality determined by bone mechanical properties.

Effect of RSG on bone structural and mechanical properties. In women, but not men, limb fractures have been reported in those taking RSG (5). Our results support this idea of compromised cortical bone strength. In our female ZF rat model, the negative effects of RSG were specific to OVX rats. No effect of RSG was observed in intact rats. Total femoral porosity was increased by >100% in the OVX RSG–treated group compared with OVX controls. This is especially important because even small increases in porosity can decrease bone strength substantially (39), and this cortical porosity is not normally seen in OVX rats. Consequently, after torsion testing of left femora, we observed decreased cortical mechanical properties (failure torque, stiffness, shear stress, and modulus) after RSG treatment. ALN treatment resulted in significantly decreased porosity as expected, owing to its antiresorptive properties. This decreased porosity in the ALN groups was reflected in the improved mechanical properties. However, these parameters did not improve to the levels seen in OVX controls, suggesting that ALN treatment does not completely prevent the decrease in mechanical properties caused by RSG treatment. Decreased bone formation may be to blame for the detrimental effects of RSG on mechanical properties in the cases where ALN is unable to completely protect against these RSG effects. In cases where ALN does exert a protective effect (for example, femoral neck fracture and three-point bending testing), an increase in bone resorption may be the cause of decreased mechanical properties after RSG treatment.

As expected, both cortical and trabecular BMD and bone mineral content (BMC) were decreased in the OVX model after RSG treatment. In a similar manner, Sottile et al. (21) performed a study with OVX, female Wistar rats and saw enhanced bone loss with RSG treatment in tibia, femur, and lumbar spine. Sorocéanu et al. (19) also observed decreased vertebral BMD and lower trabecular BV after RSG treatment in mice. In addition to our BMD analysis, our mechanical testing results suggest decreased vertebral bone strength. RSG treatment resulted in decreased ultimate load, ultimate stress, and energy to failure in the vertebrae of our female OVX model. We speculate that RSG is causing decreased strength and increased brittleness in trabecular bone of the female OVX model, resulting in an increased susceptibility to fracture. ALN treatment maintained cortical and trabecular BMD, suggesting that ALN may prevent the loss of bone mass associated with RSG treatment.

TABLE 5
Structural properties of cortical and trabecular bone for all groups

	Sham		OVX		
	Control	RSG 10	Control	RSG 10	ALN	RSG 10 + ALN
Three-point bending						
Ultimate load (N)	151.26 ± 10.12	156.16 ± 14.00	163.14 ± 17.54	154.72 ± 8.69	170.79 ± 21.68	**173.79 ± 20.12**^{cf}
Failure load (N)	150.25 ± 11.67	149.84 ± 12.80	161.13 ± 16.72	154.39 ± 8.68	169.86 ± 21.80	**169.17 ± 20.61**^{cf}
Torsion						
Failure torque (N/mm)	389.27 ± 95.35	425.59 ± 104.50	449.70 ± 93.04	**364.78 ± 97.23**^{de}	512.39 ± 124.97	**415.45 ± 106.07**^{de}
Stiffness (N/mm)	1,687.75 ± 469.61	1,926.66 ± 575.91	2,267.25 ± 636.49	**1,680.64 ± 833.62**^{de}	2,395.43 ± 514.30	**1,747.02 ± 721.45**^{e}
Vertebral compression						
Ultimate load (N)	219.03 ± 18.38	205.02 ± 30.28	181.25 ± 45.00	**146.55 ± 34.38**^{de}	**282.08 ± 58.64**^{d}	**234.59 ± 51.01**^{df}
Femoral neck fracture						
Ultimate load (N)	82.39 ± 10.70	78.63 ± 7.73	78.37 ± 10.10	**67.77 ± 10.93**^{d}	78.16 ± 11.83	**80.57 ± 10.28**^{cf}
Stiffness (N/mm)	186.63 ± 44.73	224.57 ± 42.21	205.98 ± 66.37	226.25 ± 29.22	190.11 ± 71.12	200.89 ± 1.24
Energy to failure (mJ)	25.09 ± 13.57	**18.13 ± 7.56**^{cf}	21.45 ± 6.13	16.45 ± 4.77	22.06 ± 8.06	**24.34 ± 10.63**^{cf}

Data are presented as mean ± SD. Boldface indicates significance. ^{d}Indicates significance vs. OVX controls ($P < 0.05$). ^{e}Indicates significance vs. OVX ALN group ($P < 0.05$). ^{f}Indicates significance vs. RSG 10 group ($P < 0.05$). ^{g}Indicates significance vs. Sham control group.

TABLE 6
Static and dynamic histomorphometry results for all groups

	Sham		OVX			
	Control	RSG 10	Control	RSG 10	ALN	RSG 10 + ALN
Formation						
OV/BV (%)	**0.13 ± 0.14**[d]	**0.05 ± 0.04**[d]	1.41 ± 2.54	**0.49 ± 0.45**[d]	**0.06 ± 0.07**[d]	**0.26 ± 0.59**[d]
OS/BS (%)	**0.52 ± 0.55**[d]	**0.23 ± 0.23**[d]	4.70 ± 6.34	**1.73 ± 1.61**[d]	**0.11 ± 0.13**[d]	**0.78 ± 1.88**[d]
MS (%)	8.07 ± 4.33	**6.59 ± 1.01**[d]	13.15 ± 6.28	**6.83 ± 4.09**[d]	—	—
BFR (mcm/day)	0.12 ± 0.09	**0.09 ± 0.02**[d]	0.18 ± 0.10	**0.08 ± 0.06**[d]	—	—
Resorption						
ES (%)	0.30 ± 0.22	0.51 ± 0.35	0.31 ± 0.25	**1.00 ± 0.61**[de]	0.38 ± 0.15	0.49 ± 0.21

Data are presented as mean ± SD. Boldface indicates significance. [d]Indicates significance vs. OVX controls ($P < 0.05$). [e]Indicates significance vs. OVX ALN group ($P < 0.05$).

Effect of RSG on bone formation. While TZDs such as RSG are a commonly prescribed treatment for type 2 diabetic patients, there are conflicting studies regarding the influence of RSG on bone turnover. Experimentally, in vitro, decreased bone formation after RSG treatment has been reported. PPAR-γ is a known positive adipocyte differentiation regulator; thus, activation of PPAR-γ by RSG could reduce bone formation through promotion of the adipocyte phenotype. RSG administration has been shown to decrease bone formation while also increasing adipogenesis (10,16). Our results support this evidence because histomorphometric analysis revealed decreases in bone formation parameters (OV/BV, OS/BS, and BFR) of trabecular bone in the female OVX model after RSG administration.

Effect of RSG on bone resorption. Recent in vivo studies suggest increased osteoclastogenesis due to RSG treatment. Previous studies suggest that the effect of PPAR-γ activation is specific to osteoclast genes that function along the osteoclast differentiation pathway. Wan et al. (20) discovered a pro-osteoclastogenic effect of PPAR-γ after

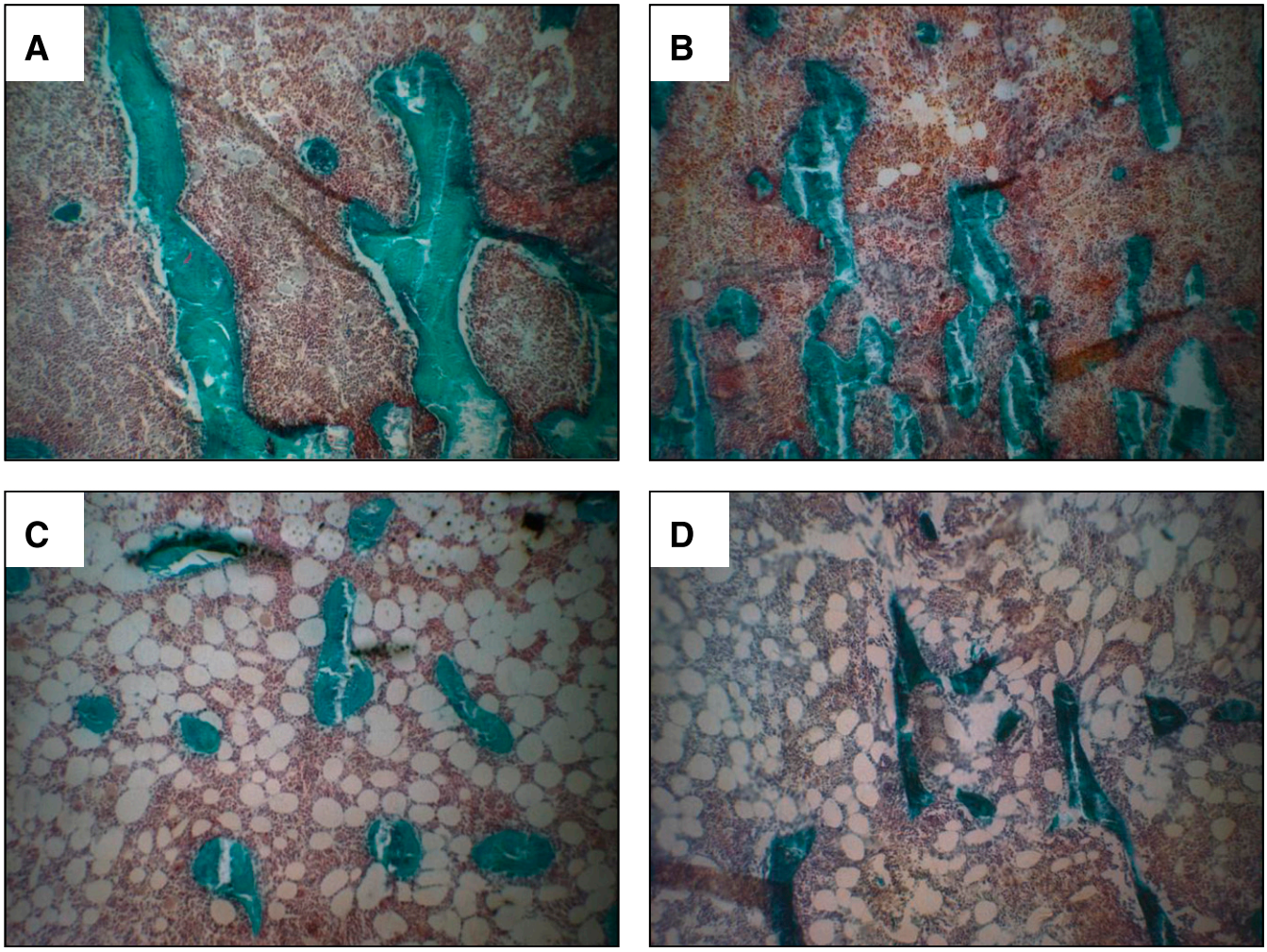

FIG. 2. Representative static histomorphometry images of rat proximal tibiae. Sections stained with Goldner's Trichrome so that trabeculae appear green and bone marrow appears pink. White space represents space occupied by adipocytes: OVX controls (*A*), OVX ALN (*B*), OVX RSG 10 (*C*), and OVX RSG 10 + ALN (*D*). (A high-quality digital representation of this figure is available in the online issue.)

RSG administration. Sottile et al. (21) also found evidence supporting increased osteoclastogenesis by reporting both an increase in marrow adipogenesis and increased bone resorption in Wistar rats after activation of PPAR-γ with RSG. Our results are consistent with these findings; we observed significantly increased ES in our model, which further suggests an increase in bone resorption. This, along with ALN's antiresorptive ability to prevent losses of trabecular architecture and bone mass, leads us to conclude that RSG significantly influences bone resorption in our rat model.

Activation of PPAR-γ can regulate c-fos levels, part of the receptor activator of nuclear factor-κB ligand signaling pathway, which can lead to increased osteoclastogenesis (19). Together, our data indicate that bone formation and bone resorption are both being affected by RSG in the female ZF OVX model. Giaginis et al. (23) also demonstrated a decrease in bone formation and increased osteoclast generation in OVX Wistar rats, whereas they saw no change in intact non-OVX rats after RSG administration.

The protective effects of estrogen and ALN on RSG-treated bone. This rat model of obesity and type 2 diabetes in combination with OVX is especially relevant because in ADOPT, increased limb fractures were reported specifically in women with type 2 diabetes. Using ALN in combination with RSG and OVX not only allowed us to examine a possible countermeasure to the deleterious effects of RSG on the skeleton but also provided insight into the mechanism by which RSG is inducing bone loss in this in vivo system. Estrogen's protection against the negative effects of RSG on bone suggests a potential mechanism by which RSG leads to bone loss. RSG activation of PPAR-γ may be interacting with receptor activator of nuclear factor-κB ligand signaling resulting in increased osteoclastogenesis and increased bone resorption. ALN, however, does not completely protect against the effects of RSG on the skeleton. In the case of three-point bending and femoral neck fracture, we have observed the ability of ALN to alleviate the effects of RSG in the female ZF rat model in vivo, whereas in torsion testing, we have not. The lack of a detectable effect in three-point bending, contrary to what we found in the torsion data, may be due to the distribution of extra porosity and the difference in the distribution of the peak stresses in the two test methods. Three-point bending causes a very small region of peak bending moment (and, therefore, stress) at the midspan of the specimen on one face of the bone. Torsion testing causes constant torque through the length of the specimen and, therefore, a much larger region of bone is equivalently stressed. This much larger region of stress results in a much higher probability of achieving failure stress at a defect (such as a pore) acting as a stress concentrator. This explains the smaller difference in means in the three-point bending data between OVX CON and OVX RSG. Since ALN is known to enhance the mechanical strength of bone through decreasing resorption and increasing mineralization, we suggest that RSG's seemingly detrimental effect on bone may be due to excess resorption in addition to decreased formation. It is important that these changes in bone remodeling have a direct effect on the mechanical properties whereby strength was decreased in both cortical and trabecular bone treated with RSG (Supplementary Fig. 1). This finding has significant implications for women taking this drug.

Potential impact of diabetes. While this study was carried out in the ZF *fa/fa* rat model of obesity, associated with insulin resistance and glucose intolerance, it should be noted that the diabetes state itself has been documented to have adverse effects on bone characteristics (11). We examined the effects of RSG in this context since the TZD drugs are administered to human subjects with type 2 diabetes. While some rodent studies of RSG effects in nondiabetic rats (14) suggest similar effects, a direct comparison would be interesting to explore the interacting effects of RSG and diabetes on bone.

One other potential caveat is that RSG treatment may improve the diabetes state. Since, as noted above, diabetes may adversely affect bone, such an effect of RSG would underestimate its adverse effects. We have measured random morning-fed glucose values in the different groups of rats at baseline and over the 3 months of treatment (Supplementary Table 2). By two-way repeated-measures ANOVA, there were no significant differences in any of the glucose values and no interaction detected between treatment groups and time. There was a trend toward lower mean glucose in the OVX group treated with RSG from baseline to 3 months, which was not seen in the combination RSG plus ALN-treated group. This was not likely significant and if so, would have caused an underestimation of the benefit of ALN. However, there is no evidence in human subjects with diabetes treated with bisphosphonates that glycemic control is altered (46,47). Taken together, these data indicate that the antidiabetes effects of RSG and the diabetes state itself are not significant confounders of the RSG actions on bone.

In conclusion, we found that RSG treatment enhanced the effects of OVX on bone loss in cortical and trabecular bone in the female OVX ZF model. Congruent with this bone loss were decreased mechanical properties in both cortical and trabecular bone after RSG treatment. ALN appeared to prevent the bone loss caused by RSG and partially prevented decreases in mechanical strength of cortical and trabecular bone. RSG treatment appeared to cause decreased bone formation as well as large increases in bone resorption, suggesting a possible mechanism by which RSG induces bone loss and inferior bone quality in our OVX female model. Especially interesting is the increased long bone porosity after RSG treatment, which may explain the increased susceptibility to limb fractures experienced by postmenopausal women taking RSG. Further examination into the proresorptive capabilities of RSG should be carried out to confirm the influence that PPAR-γ activation by RSG is having on bone resorption versus bone formation.

ACKNOWLEDGMENTS

L.D.S. has received funding from the Canadian Institutes of Health Research (CIHR) and the Banting and Best Diabetes Center at the University of Toronto. I.G.F. and M.D.G. have received funding from the CIHR and GlaxoSmithKline. No other potential conflicts of interest relevant to this article were reported.

L.D.S. conducted experimental work, analyzed data, and wrote the manuscript. R.R. contributed to the animal experiment. T.L.W. contributed to experimental work (mechanical testing and MicroCT) and wrote the manuscript. I.G.F. contributed to the design of the experiment and wrote the manuscript. M.D.G. designed and supervised the experiment and wrote the manuscript.

The authors thank Mr. Richard Cheung, Samuel Lunenfeld Research Institute, Mount Sinai Hospital; Dr. David Cole, Womens College, Women's College Hospital, Toronto, Ontario, Canada; Dr. Reinhold Vieth, Mount Sinai Hospital;

Mr. Doug Holmyard, Mount Sinai Hospital; and Dr. Mircea Dumitriu, Samuel Lunenfeld Research Institute, Mount Sinai Hospital, for their help.

REFERENCES

1. Zimmet P, Alberti KG, Shaw J. Global and societal implications of the diabetes epidemic. Nature 2001;414:782–787
2. Natali A, Baldeweg S, Toschi E, et al. Vascular effects of improving metabolic control with metformin or rosiglitazone in type 2 diabetes. Diabetes Care 2004;27:1349–1357
3. Walker AB, Chattington PD, Buckingham RE, Williams G. The thiazolidinedione rosiglitazone (BRL-49653) lowers blood pressure and protects against impairment of endothelial function in Zucker fatty rats. Diabetes 1999;48: 1448–1453
4. Schwartz AV, Sellmeyer DE, Vittinghoff E, et al. Thiazolidinedione use and bone loss in older diabetic adults. J Clin Endocrinol Metab 2006;91: 3349–3354
5. Gruntmanis U, Fordan S, Ghayee HK, et al. The peroxisome proliferator-activated receptor-gamma agonist rosiglitazone increases bone resorption in women with type 2 diabetes: a randomized, controlled trial. Calcif Tissue Int 2010;86:343–349
6. Berberoglu Z, Yazici AC, Demirag NG. Effects of rosiglitazone on bone mineral density and remodelling parameters in postmenopausal diabetic women: a 2-year follow-up study. Clin Endocrinol (Oxf) 2010;73:305–312
7. Douglas IJ, Evans SJ, Pocock S, Smeeth L. The risk of fractures associated with thiazolidinediones: a self-controlled case-series study. PLoS Med 2009;6:e1000154
8. Mancini T, Mazziotti G, Doga M, et al. Vertebral fractures in males with type 2 diabetes treated with rosiglitazone. Bone 2009;45:784–788
9. Viberti G, Kahn SE, Greene DA, et al. A Diabetes Outcome Progression Trial (ADOPT): an international multicenter study of the comparative efficacy of rosiglitazone, glyburide, and metformin in recently diagnosed type 2 diabetes. Diabetes Care 2002;25:1737–1743
10. Lin TH, Yang RS, Tang CH, Lin CP, Fu WM. PPARgamma inhibits osteogenesis via the down-regulation of the expression of COX-2 and iNOS in rats. Bone 2007;41:562–574
11. Rzonca SO, Suva LJ, Gaddy D, Montague DC, Lecka-Czernik B. Bone is a target for the antidiabetic compound rosiglitazone. Endocrinology 2004; 145:401–406
12. Cheng AY, Fantus IG. Oral antihyperglycemic therapy for type 2 diabetes mellitus. CMAJ 2005;172:213–226
13. Lehmann JM, Moore LB, Smith-Oliver TA, Wilkison WO, Willson TM, Kliewer SA. An antidiabetic thiazolidinedione is a high affinity ligand for peroxisome proliferator-activated receptor gamma (PPAR gamma). J Biol Chem 1995;270:12953–12956
14. Tornvig L, Mosekilde LI, Justesen J, Falk E, Kassem M. Troglitazone treatment increases bone marrow adipose tissue volume but does not affect trabecular bone volume in mice. Calcif Tissue Int 2001;69:46–50
15. Okuno A, Tamemoto H, Tobe K, et al. Troglitazone increases the number of small adipocytes without the change of white adipose tissue mass in obese Zucker rats. J Clin Invest 1998;101:1354–1361
16. Okazaki R, Toriumi M, Fukumoto S, et al. Thiazolidinediones inhibit osteoclast-like cell formation and bone resorption in vitro. Endocrinology 1999;140:5060–5065
17. Ali AA, Weinstein RS, Stewart SA, Parfitt AM, Manolagas SC, Jilka RL. Rosiglitazone causes bone loss in mice by suppressing osteoblast differentiation and bone formation. Endocrinology 2005;146:1226–1235
18. Schwartz AV. Diabetes mellitus: Does it affect bone? Calcif Tissue Int 2003; 73:515–519
19. Sorocéanu MA, Miao D, Bai XY, Su H, Goltzman D, Karaplis AC. Rosiglitazone impacts negatively on bone by promoting osteoblast/osteocyte apoptosis. J Endocrinol 2004;183:203–216
20. Wan Y, Chong LW, Evans RM. PPAR-gamma regulates osteoclastogenesis in mice. Nat Med 2007;13:1496–1503
21. Sottile V, Seuwen K, Kneissel M. Enhanced marrow adipogenesis and bone resorption in estrogen-deprived rats treated with the PPARgamma agonist BRL49653 (rosiglitazone). Calcif Tissue Int 2004;75:329–337
22. Lazarenko OP, Rzonca SO, Hogue WR, Swain FL, Suva LJ, Lecka-Czernik B. Rosiglitazone induces decreases in bone mass and strength that are reminiscent of aged bone. Endocrinology 2007;148:2669–2680
23. Giaginis C, Tsantili-Kakoulidou A, Theocharis S. Peroxisome proliferator-activated receptors (PPARs) in the control of bone metabolism. Fundam Clin Pharmacol 2007;21:231–244
24. Hill PA. Bone remodelling. Br J Orthod 1998;25:101–107
25. Eriksen EF, Hodgson SF, Eastell R, Cedel SL, O'Fallon WM, Riggs BL. Cancellous bone remodeling in type I (postmenopausal) osteoporosis: quantitative assessment of rates of formation, resorption, and bone loss at tissue and cellular levels. J Bone Miner Res 1990;5:311–319
26. Cowin SC. *Bone Biomechanics Handbook.* Boca Raton, FL, CRC Press, 2001
27. Watts NB. Treatment of osteoporosis with bisphosphonates. Endocrinol Metab Clin North Am 1998;27:419–439
28. Bray GA. The Zucker-fatty rat: a review. Fed Proc 1977;36:148–153
29. Zucker LM. Efficiency of energy utilization by the Zucker hereditarily obese rat "fatty" (38569). Proc Soc Exp Biol Med 1975;148:498–500
30. Zucker LM, Antoniades HN. Insulin and obesity in the Zucker genetically obese rat "fatty." Endocrinology 1972;90:1320–1330
31. Kasiske BL, O'Donnell MP, Keane WF. The Zucker rat model of obesity, insulin resistance, hyperlipidemia, and renal injury. Hypertension 1992;19 (Suppl.):I110–I115
32. Schirardin H, Bach A, Schaeffer A, Bauer M, Weryha A. Biological parameters of the blood in the genetically obese Zucker rat. Arch Int Physiol Biochim 1979;87:275–289
33. An YH, Martin KL. *Handbook of Histology Methods for Bone and Cartilage.* Totowa, NJ, Humana Press Inc., 2003
34. Nagy TR, Prince CW, Li J. Validation of peripheral dual-energy X-ray absorptiometry for the measurement of bone mineral in intact and excised long bones of rats. J Bone Miner Res 2001;16:1682–1687
35. Thomsen JS, Laib A, Koller B, Prohaska S, Mosekilde LI, Gowin W. Stereological measures of trabecular bone structure: comparison of 3D micro computed tomography with 2D histological sections in human proximal tibial bone biopsies. J Microsc 2005;218:171–179
36. Kasra M, Vanin CM, MacLusky NJ, Casper RF, Grynpas MD. Effects of different estrogen and progestin regimens on the mechanical properties of rat femur. J Orthop Res 1997;15:118–123
37. Turner CH, Hsieh YF, Müller R, et al. Genetic regulation of cortical and trabecular bone strength and microstructure in inbred strains of mice. J Bone Miner Res 2000;15:1126–1131
38. Chachra D, Kasra M, Vanin CM, MacLusky NJ, Casper RF, Grynpas MD. The effect of different hormone replacement therapy regimens on the mechanical properties of rat vertebrae. Calcif Tissue Int 1995;56:130–134
39. Peng ZQ, Väänänen HK, Zhang HX, Tuukkanen J. Long-term effects of ovariectomy on the mechanical properties and chemical composition of rat bone. Bone 1997;20:207–212
40. Turner CH. Biomechanics of bone: determinants of skeletal fragility and bone quality. Osteoporos Int 2002;13:97–104
41. Holmes C, Khan TS, Owen C, Ciliberti N, Grynpas MD, Stanford WL. Longitudinal analysis of mesenchymal progenitors and bone quality in the stem cell antigen-1-null osteoporotic mouse. J Bone Miner Res 2007;22: 1373–1386
42. Parfitt AM, Drezner MK, Glorieux FH, et al. Bone histomorphometry: standardization of nomenclature, symbols, and units. Report of the ASBMR Histomorphometry Nomenclature Committee. J Bone Miner Res 1987;2: 595–610
43. Sloan AV, Martin JR, Li S, Li J. Parathyroid hormone and bisphosphonate have opposite effects on stress fracture repair. Bone 2010;47:235–240
44. Allen MR, Burr DB. Three years of alendronate treatment results in similar levels of vertebral microdamage as after one year of treatment. J Bone Miner Res 2007;22:1759–1765
45. Arlot M, Meunier PJ, Boivin G, et al. Differential effects of teriparatide and alendronate on bone remodeling in postmenopausal women assessed by histomorphometric parameters. J Bone Miner Res 2005;20: 1244–1253
46. Keegan TH, Schwartz AV, Bauer DC, Sellmeyer DE, Kelsey JL; Fracture Intervention Trial. Effect of alendronate on bone mineral density and biochemical markers of bone turnover in type 2 diabetic women: the Fracture Intervention Trial. Diabetes Care 2004;27:1547–1553
47. Rocha M, Nava LE, Vázquez de la Torre C, Sánchez-Márin F, Garay-Sevilla ME, Malacara JM. Clinical and radiological improvement of periodontal disease in patients with type 2 diabetes mellitus treated with alendronate: a randomized, placebo-controlled trial. J Periodontol 2001; 72:204–209